Catalysis Today 175 (2011) 223–230

Contents lists available at ScienceDirect

Catalysis Today

journal homepage: www.elsevier.com/locate/cattod

The durability of alumina supported Pd catalysts for the combustion of methane in the presence of SO_2

Xuehong Zi, Licheng Liu, Bin Xue, Hongxing Dai, Hong He*

Laboratory of Catalysis Chemistry and Nanoscience, Department of Chemistry and Chemical Engineering, College of Environmental and Energy Engineering, Beijing University of Technology, Beijing 100124, China

ARTICLE INFO

Article history:
Received 20 October 2010
Received in revised form 9 March 2011
Accepted 16 March 2011
Available online 5 May 2011

Keywords:
Sulfur poisoning
Sulfur accumulation
Methane combustion
Palladium catalysts

ABSTRACT

In the present work, the 1.0 wt% Pd/γ-Al_2O_3, 1.0 wt% Pd/10 wt% CeO_2/γ-Al_2O_3 and 1.0 wt% Pd/10 wt% $Ce_{0.6}Zr_{0.4}O_2$/γ-Al_2O_3 catalysts were prepared and used for the catalytic combustion of methane. The durabilities of the three catalysts were investigated based on the phenomena of SO_2 poisoning in methane catalytic combustion. The presence of SO_2 in the reaction gases resulted in an increase of 70–250 °C in light-off temperature for methane conversion over all the catalysts. The sulfates could be formed below and decomposed above 600–700 °C in the reaction over the catalysts, which led to the inhibition and recovery of the catalytic activity, respectively. The introduction of CeO_2 or $Ce_{0.6}Zr_{0.4}O_2$ decreased the decomposition temperature of sulfates by 50–100 °C. Sulfur accumulation on the catalyst surface was investigated by sulfur content analysis and TG measurements after pretreatment with SO_2. The saturated sulfur contents were all about 5 wt% for the three catalysts. In spite of sulfur poisoning, no obvious changes in the particle morphologies and sizes were observed for the fresh and used catalysts.

1. Introduction

Catalytic combustion of methane has been intensively investigated in the past decades due to its practical applications in pollutant abatement and power generation. It is a "green" technology for methane combustion because of its possibility of producing heat and energy at relative low temperature with ultra-low emissions of NO_x, CO, and hydrocarbons (HC) than conventional non-catalytic combustions [1–3]. The supported Pd catalysts appear to be active for the combustion of natural gas under lean conditions [4,5]. Alumina is a support used intensively and ceria is reported to be beneficial for the enhancement in methane combustion activity of supported metal catalysts [6–9]. Another previous work revealed that palladium supported on ZrO_2 showed better performance than that supported on other supports under the reaction conditions adopted by the authors [10]. The CeO_2–ZrO_2 mixed oxides have also been used as supports to disperse noble metals and subsequently act as catalysts for methane combustion [11]. No matter what support or catalyst is used, the big challenge for the catalytic combustion of methane is to avoid deactivation of the catalysts. Generally speaking, Pd catalysts can be deactivated due to the sintering of support [12], the loss of active phase [13], and the poisoning of sulfur [14–17].

It has been demonstrated in previous studies that sulfur compounds play a key role in the deactivation of the catalysts used for methane combustion [14,16]. Many researchers [15–23] have examined the effects of sulfur poisoning on the performance of Pd catalysts. The influences of sulfur compound concentration, water in the feed, and nature of the support on the sulfur poisoning have been also widely explored. Sulfur-containing compounds were shown to be readily converted into SO_x that strongly adsorbed as stable sulfate species on the surfaces of PdO particles. The number of active sites decreased until the saturation of the active site surfaces by sulfate species, resulting in the complete loss of catalytic activity for methane oxidation. Hoyos et al. [17] examined the influence of support (γ-Al_2O_3 and SiO_2) nature on the poisoning of Pd catalysts by introducing 100 ppm H_2S to the methane combustion system. Both of the catalysts exhibited serious deactivation in the presence of sulfur and the rate of deactivation was dependent on the support. The low deactivation rate of the γ-Al_2O_3 supported Pd catalyst was attributed to the larger capacity of alumina that could trap sulfates and sulfites since H_2S was fully oxidized to SO_2/SO_3 under the reaction conditions. The mechanism for the deactivation of Pd catalysts by sulfur oxides in lean burn environments was investigated by Lampert et al. [19], who proposed that SO_2 was first converted into SO_3 and then the latter was adsorbed as sulfates on the PdO surface. The extent of sulfur poisoning over the Pd catalysts loaded on the sulfated supports was less than the Pd catalysts loaded on other supports, this phenomenon was attributed to the adsorption of SO_3 over the support.

* Corresponding author. Tel.: +86 10 6739 6588; fax: +86 10 6739 6588.
E-mail address: hehong@bjut.edu.cn (H. He).

0920-5861/$ – see front matter © 2011 Elsevier B.V. All rights reserved.
doi:10.1016/j.cattod.2011.03.039

The regeneration of sulfur-poisoning supported Pd catalysts is another important issue for methane combustion. Ordóñez et al. [23] investigated the regeneration of a deactivated $Pd/\gamma\text{-}Al_2O_3$ catalyst in the presence of SO_2. They reported that the deactivated $Pd/\gamma\text{-}Al_2O_3$ catalyst could be recovered by H_2 treatment that was one of the most efficient ways for deactivated catalyst regeneration. In general, the sharply deactivated Pd catalysts at low temperature are relatively easy to be regenerated.

As mentioned above, the sulfur-poisoning phenomenon of supported Pd catalysts at relatively low temperatures has been investigated by many researchers [23–25]. However, the residue and accumulation of sulfur species over the methane combustion catalysts at elevated temperatures remain unclear. The aim of the present study is to investigate the sulfur poisoning and deactivation mechanisms of the Pd catalysts supported on $\gamma\text{-}Al_2O_3$, $CeO_2/\gamma\text{-}Al_2O_3$, and $CeO_2\text{–}ZrO_2/\gamma\text{-}Al_2O_3$ for the combustion of methane, and to probe the deactivation mechanism, especially the accumulation of sulfur species on the surfaces of the catalysts at relatively high temperatures. In addition, the effects of sulfur accumulation after the sulfur poisoning at high temperature on catalytic performance were also examined.

2. Experimental

2.1. Catalyst preparation

The 10 wt% $CeO_2/\gamma\text{-}Al_2O_3$ and 10 wt% $Ce_{0.6}Zr_{0.4}O_2/\gamma\text{-}Al_2O_3$ catalysts were prepared as follows. The $ZrO(NO_3)_2{\cdot}2H_2O$ (Sinopharm Chemical Reagent Beijing Co., Ltd., >99%) and/or $Ce(NO_3)_3{\cdot}6H_2O$ (Sinopharm Chemical Reagent Beijing Co., Ltd., >99%) with the appropriate quantities were dissolved in deionized water. An appropriate amount of $\gamma\text{-}Al_2O_3$ (Zhejiang Ultrafine Powders & Chemicals Company, 200 $m^2\,g^{-1}$) was added to the above solution. The mixture was dispersed via ultrasonic irradiation under stirring and then dried at 120 °C for 24 h. The samples were calcined at 550 °C in air and well ground, yielding 10 wt% $CeO_2/\gamma\text{-}Al_2O_3$ and 10 wt% $Ce_{0.6}Zr_{0.4}O_2/\gamma\text{-}Al_2O_3$. The 1.0 wt% $Pd/\gamma\text{-}Al_2O_3$, 1.0 wt% Pd/10 wt% $CeO_2/\gamma\text{-}Al_2O_3$, and 1.0 wt% Pd/10 wt% $Ce_{0.6}Zr_{0.4}O_2/\gamma\text{-}Al_2O_3$ catalysts were prepared by impregnating the $\gamma\text{-}Al_2O_3$, $CeO_2/\gamma\text{-}Al_2O_3$ or $Ce_{0.6}Zr_{0.4}O_2/\gamma\text{-}Al_2O_3$ powders with the appropriate concentration of $Pd(NO_3)_2{\cdot}2H_2O$ solution, respectively. The solids were calcined in air at 550 °C and in turn ground, tableted, crushed, and sieved to a size range of 40–60 mesh before use.

2.2. Catalytic evaluation

The activities of the catalysts for the combustion of methane were measured in a fixed-bed quartz micro-reactor (i.d. = 8 mm) at atmospheric pressure. The catalyst (90 mg) was packed in the middle of the reactor between two quartz wool plugs. The reaction temperature was monitored by a thermocouple located at the middle of the catalyst bed and regulated from 200 to 800 °C at an interval of 50 °C. The flow rate of reactant mixture (2% CH_4 + 8% O_2 + 90% N_2 (balance)), in the absence or presence of 200 ppm SO_2, was controlled by mass flow regulators supplied by Beijing Seven Star Electronics Co., Ltd. (D07-7B). The space velocity (SV) was ca. 50,000 h^{-1}. The concentrations of CO, CO_2, O_2, and CH_4 in the outlet of the reactor were determined by a gas chromatograph (SHIMADZU GC-14C) equipped with a thermal conductivity detector and a 5A molecular sieve packing column. For the SO_2-poisoning pretreatment, the catalysts were heated to 500 °C in a flow of 5% SO_2/N_2 (v/v, 50 ml min^{-1}) and maintained at this temperature for 1.5, 5 or 24 h before the catalytic test.

To examine the catalytic performance of the $Pd/CeO_2/\gamma\text{-}Al_2O_3$ catalyst after thermal treatment at high temperature, the catalyst was calcined at 1200 °C for 100, 200 or 300 h. The activity was evaluated using a mixture of 2% CH_4, 10% O_2, and N_2 (balance) in a total flow of 200 ml min^{-1} and at a space velocity of 20,000 h^{-1}.

2.3. Characterization

The crystal structures of the catalysts were determined by an X-ray diffractometer (Bruker/AXS D8 Advance), operating at 50 kV and 50 mA with Cu Kα radiation. The patterns were referred to the powder diffraction files – 1998 ICDD PDF Database for the identification. The specific surface areas of the catalysts were measured by nitrogen adsorption at −196 °C on a Micromeritics ASAP 2020 apparatus. The TEM images of the fresh and poisoned catalysts were recorded with a JEM 2010 (JOEL) operated at 100 kV.

The SO_2-TPD experiments were carried out in a similar kind of micro-reactor. For pretreatment, 100 mg of the sample was heated to 500 °C in a flow of 5% O_2/N_2 (v/v, 50 ml min^{-1}) or 5% H_2/N_2 (v/v, 50 ml min^{-1}) and maintained at this temperature for 1 h before being purged with a mixture of 5% SO_2/N_2 (v/v, 50 ml min^{-1}) at 500 °C for 1.5 h. After being cooled to room temperature under the same atmosphere, the sample was treated in a flow of helium (50 ml min^{-1}) to clean the catalysts surface, and then heated from 30 to 900 °C at a ramp of 15 °C min^{-1}. The effluent gases (SO_2, SO_3, and O_2) were monitored on-line by a mass spectrometer (Hiden HPR 20).

X-ray photoelectron spectroscopic (XPS) spectra were collected on a Kratos Analytical Axis Ultra spectrometer with a Al Kα source ($h\nu$ = 1486.71 eV). The binding energy of C 1s at 284.6 eV was used as the reference for binding energy calibration. Thermogravimetric (TG) analyses of the samples were conducted on a STD Q600 instrument (TA). The sulfur contents in the catalysts were analyzed by a Sulfur–Carbon analyzer (Horiba).

3. Results and discussion

3.1. Activities of the fresh and SO_2-poisoned catalysts for methane combustion

The activities of the 1.0 wt% $Pd/\gamma\text{-}Al_2O_3$, 1.0 wt% Pd/10 wt% $CeO_2/\gamma\text{-}Al_2O_3$, and 1.0 wt% Pd/10 wt% $Ce_{0.6}Zr_{0.4}O_2/\gamma\text{-}Al_2O_3$ catalysts for methane combustion were examined in the absence or presence of 200 ppm SO_2 in reactant feed and are shown in Fig. 1.

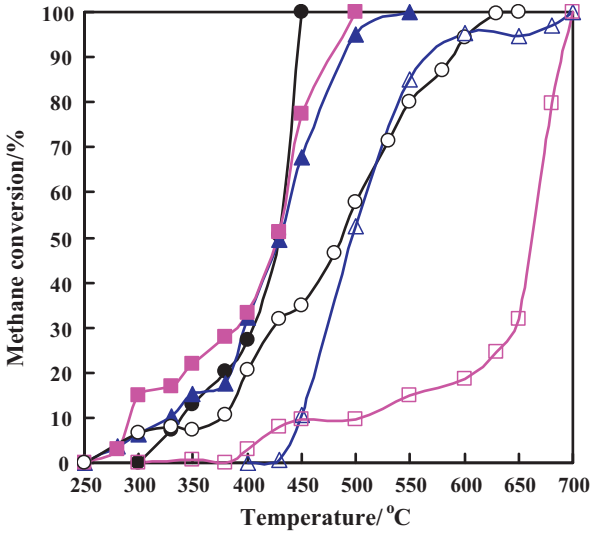

Fig. 1. Methane conversion over (●, ○) $Pd/\gamma\text{-}Al_2O_3$, (▲, △) $Pd/CeO_2/\gamma\text{-}Al_2O_3$, (■, □) $Pd/Ce_{0.6}Zr_{0.4}O_2/\gamma\text{-}Al_2O_3$. Filled and open symbols represent the activity in the absence or presence of 200 ppm SO_2 in reaction feed, respectively.

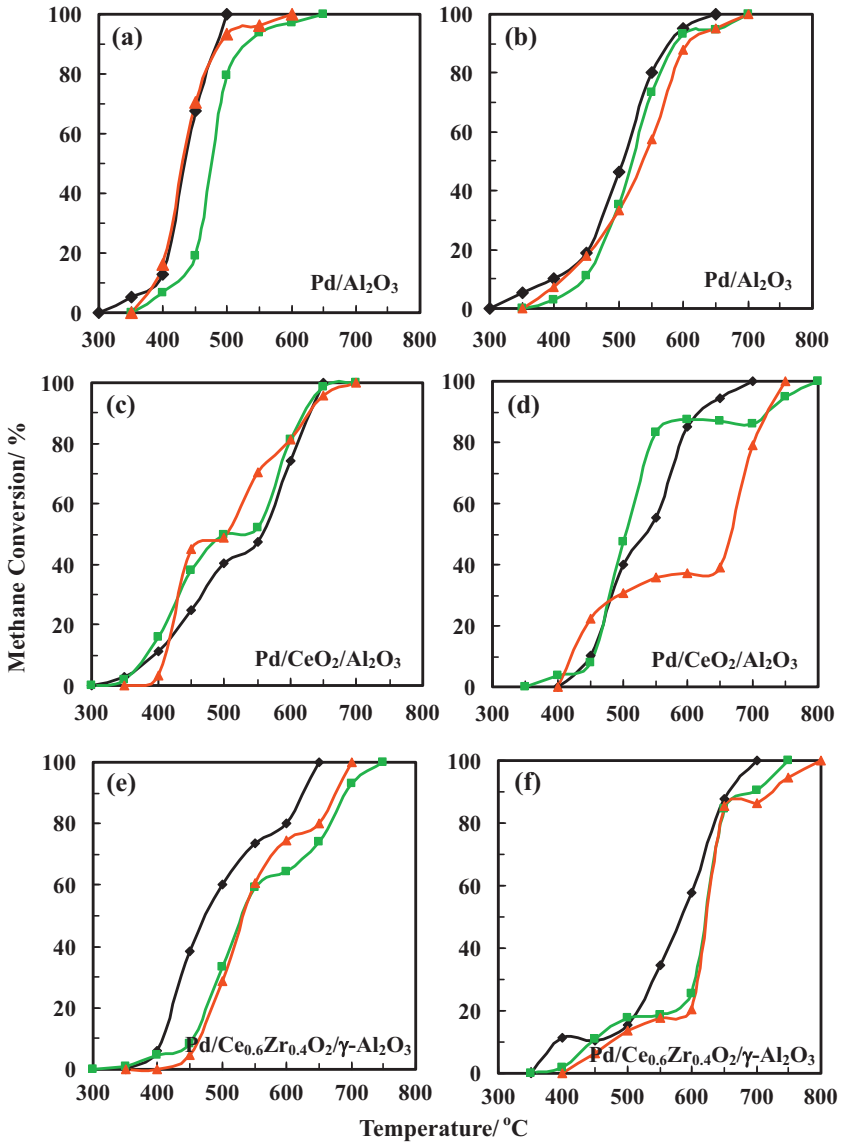

Fig. 2. Methane conversion over the catalysts pretreated by SO_2 for (♦) 1.5 h, (■) 5 h, (▲) 24 h in the (a, c, e) absence or (b, d, f) presence of 200 ppm SO_2.

In the absence of SO_2, the three catalysts exhibited similar catalytic activities. The light-off temperature (T_{50}) was ca. 430 °C, in agreement with the results previously reported by other researchers [13]. For all of the catalysts, methane combustion activity decreased in the presence of SO_2, the light-off temperatures were 485, 495, and 660 °C over the 1.0 wt% Pd/γ-Al_2O_3, 1.0 wt% Pd/10 wt% CeO_2/γ-Al_2O_3, and 1.0 wt% Pd/10 wt% $Ce_{0.6}Zr_{0.4}O_2$/γ-Al_2O_3 catalysts, respectively. This indicates that the presence of SO_2 in the reaction system had a significant negative effect on the activities of the supported Pd catalysts for methane combustion. Especially, the catalytic activity of the CeO_2- or $Ce_{0.6}Zr_{0.4}O_2$-containing catalyst decreased greatly, suggesting the weak SO_2 tolerance of those catalysts.

Fig. 2 shows the catalytic activities in the presence and absence of 200 ppm SO_2 for methane combustion over the catalysts poisoned in a mixture of 5% SO_2–95% N_2 (v/v, 50 ml min^{-1}) for 1.5, 5, and 24 h, respectively. Compared to the fresh catalysts (Fig. 1), the SO_2-poisoned catalysts exhibited a deactivation in the catalytic activity of methane combustion in the both cases of presence and absence of SO_2. In the absence of SO_2, no significant change of T_{50} was observed over the 1.0 wt% Pd/γ-Al_2O_3 catalyst, but the T_{100} was ca. 100 °C higher over the SO_2-poisoned catalyst than over the fresh one. The SO_2-poisoned 1.0 wt% Pd/10 wt% CeO_2/γ-Al_2O_3 and 1.0 wt% Pd/10 wt% $Ce_{0.6}Zr_{0.4}O_2$/γ-Al_2O_3 catalysts showed significant declines in catalytic activity compared to the fresh catalysts. Methane combustion activities of 1.0 wt% Pd/γ-Al_2O_3 and 1.0 wt% Pd/10 wt% $Ce_{0.6}Zr_{0.4}O_2$/γ-Al_2O_3 decreased slightly as the SO_2-poisoning time increased to 5 or 24 h. One should pay attention on that a reaction plateau in the temperature range from 450 to 550 °C was observed on the catalytic activity curve over 1.0 wt% Pd/10 wt% CeO_2/γ-Al_2O_3 sample. As for the 1.0 wt% Pd/10 wt% $Ce_{0.6}Zr_{0.4}O_2$/γ-Al_2O_3 catalyst, the reaction plateau was located between 550 and 650 °C. The phenomena could be explained that the sulfur species were formed on the surface of the catalysts at the temperature range from 450 to 650 °C in the forms of $Al_2(SO_4)_3$, $Ce_2(SO_4)_3$, $Ce(SO_4)_2$, and $Zr(SO_4)_2$. With the rise in temperature, the catalytic activity was recovered and increased after the plateau due to the decomposition of the sulfates. It was further proved by the results of the SO_2-TPD studies. This phenomenon could be attributed to the reason that the transfer of sulfur species from the support to PdO active sites occurred more easily over the Pd/CeO_2/Al_2O_3 and Pd/$Ce_{0.6}Zr_{0.4}O_2$/Al_2O_3 catalysts than over the Pd/Al_2O_3 sam-

ple, yielding a suppression on catalytic activity for the former two catalysts. Another possible reason could be that the redox process of Pd ↔ PdO was hindered by the sulfur species that could not release O atom to Pd to form PdO, which was claimed to be the active center for methane combustion. As the reaction temperature increased, the sulfur species on the surfaces of catalysts would decompose, leading to the regeneration of active centers, and then the catalytic activity recovered. On the contrary, one cannot observe the reaction plateau on the activity curve of 1.0 wt% Pd/γ-Al_2O_3, suggesting that sulfur species attributed to reaction plateau were mainly formed on CeO_2 and $Ce_{0.6}Zr_{0.4}O_2$. The transfer of sulfur species from the surface of CeO_2 and $Ce_{0.6}Zr_{0.4}O_2$ to PdO was easier than the deposition of sulfur species on PdO. It was also difficulty for the sulfur species to transfer from the surface of Al_2O_3 to the PdO due to the stability of $Al_2(SO_4)_3$. Therefore, the methane combustion activity of 1.0 wt% Pd/10 wt% CeO_2/γ-Al_2O_3 and 1.0 wt% Pd/10 wt% $Ce_{0.6}Zr_{0.4}O_2$/γ-Al_2O_3 was lower than that of 1.0 wt% Pd/γ-Al_2O_3 after SO_2 treatment.

In the presence of SO_2 in reaction system, the light-off temperature for methane combustion over the SO_2-poisoned 1.0 wt% Pd/Al_2O_3 catalyst decreased to ca. 530 °C and the total oxidation temperature was ca. 700 °C. As for the 1.0 wt% Pd/10 wt% CeO_2/γ-Al_2O_3 and 1.0 wt% Pd/10 wt% $Ce_{0.6}Zr_{0.4}O_2$/γ-Al_2O_3 catalysts pretreated in a mixture of 5% SO_2–95% N_2 (v/v, 50 ml min^{-1}) for 1.5, 5 or 24 h, we observed serious SO_2-poisoning phenomena that methane combustion activities were suppressed largely. Especially for the SO_2-poisoned 1.0 wt% Pd/10 wt% $Ce_{0.6}Zr_{0.4}O_2$/γ-Al_2O_3 catalyst, the catalytic activity increased very slowly in the range of 300–600 °C. However, a sharp increase in methane conversion was observed above 600 °C. As the SO_2-poisoning time increased to 5 and 24 h, two reaction plateaus were observed in the temperature ranging from 550 to 700 °C (85% methane conversion) and from 500 to 650 °C (35% methane conversion) on the catalytic activity curve over 1.0 wt% Pd/10 wt% CeO_2/γ-Al_2O_3 catalyst, respectively. And the recovery and sharp increase in catalytic activity were resulted from the decomposition of sulfates.

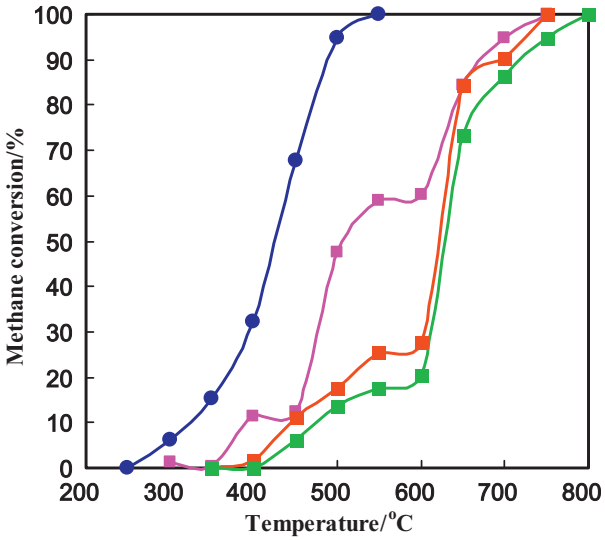

Fig. 3. Catalytic activities of Pd/CeO_2/(-Al_2O_3 after methane catalytic combustion at 1200 °C for (●) 0 h, (♦) 100 h, (■) 200 h, and (▲) 300 h.

In order to investigate the durability of the catalysts, methane catalytic combustion at 1200 °C in the presence of 200 ppm SO_2 over the 1.0 wt% Pd/10 wt% CeO_2/γ-Al_2O_3 catalyst was carried out for 0, 100, 200 or 300 h. After the reaction, the light-off behavior of the 1.0 wt% Pd/10 wt% CeO_2/γ-Al_2O_3 catalyst was studied, and the results are presented in Fig. 3. The light-off temperature of the fresh 1.0 wt% Pd/10 wt% CeO_2/γ-Al_2O_3 catalyst was ca. 430 °C, whereas for the catalyst after methane combustion for 100, 200, and 300 h at 1200 °C, the light-off temperatures increased to 506, 620 and 628 °C, respectively. From the experimental data, one can see that after the methane reaction of 100 and 200 h at 1200 °C, the catalytic activity of 1.0 wt% Pd/10 wt% CeO_2/γ-Al_2O_3 decreased markedly. As the reaction time increased to 300 h, no observable change in light-off temperature appeared in the light-off characteristic curve as

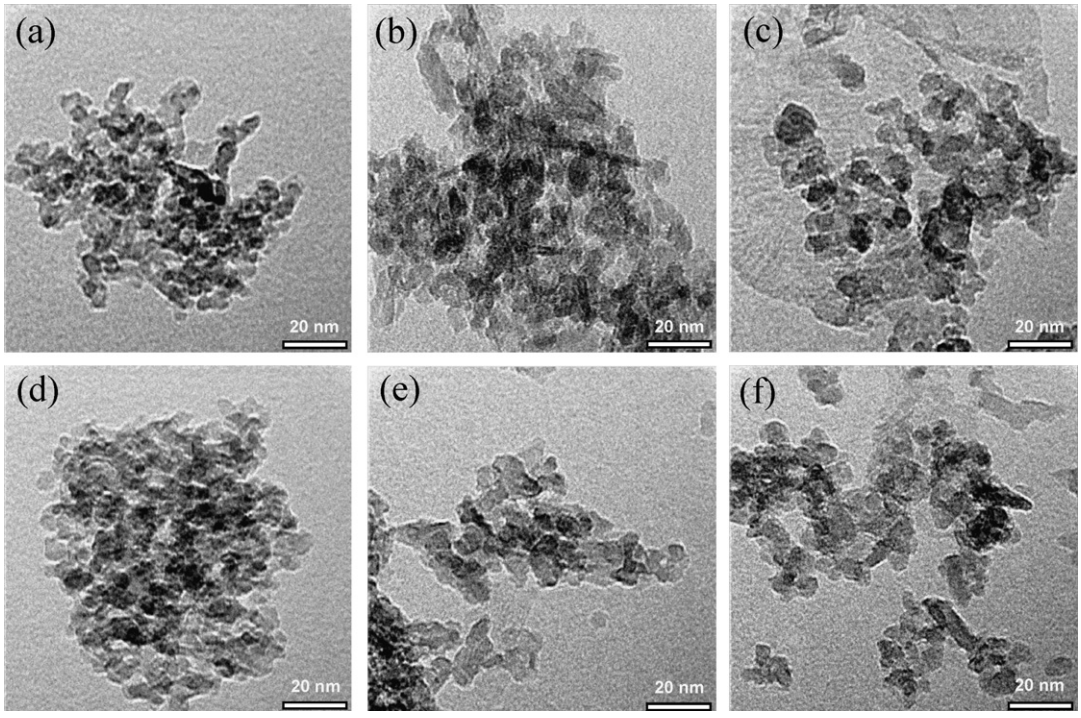

Fig. 4. TEM images of the (a–c) fresh and (d–f) SO_2-tretaed Pd/γ-Al_2O_3 (a, d), Pd/CeO_2/γ-Al_2O_3 (b, e), Pd/$Ce_{0.6}Zr_{0.4}O_2$/γ-Al_2O_3 (c, f) catalysts.

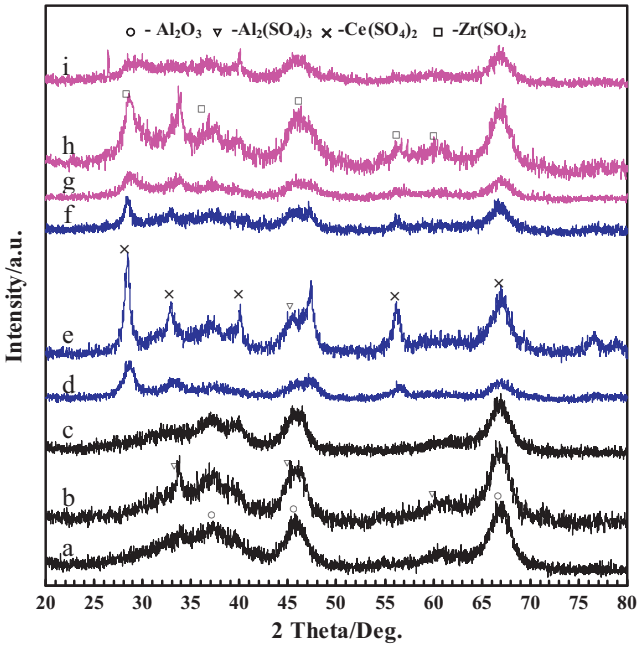

Fig. 5. XRD patterns of (a–c) Pd/Al_2O_3 (d–f) $Pd/CeO_2/Al_2O_3$, and (g–i) $Pd/CeZrO_2/Al_2O_3$ before (a, d, g) and after (b, e, h) catalytic combustion of methane in the presence of 200 ppm SO_2 and after (c, f, i) SO_2-TPD.

compared to the sample after catalytic reaction of 200 h, indicating that the 1.0 wt% Pd/10 wt% CeO_2/γ-Al_2O_3 catalyst became stable after methane combustion at 1200 °C for 200 h and the activity of the catalyst was also high enough to meet the requirement for the methane catalytic combustion. The sharp increase in activity was also observed clearly for the aged catalysts as the reaction temperature was higher than 600 °C. The sulfates decomposed at the relative high temperature could be formed in the catalytic combustion of methane in the presence of 200 ppm SO_2, leading to the deactivation of the catalysts.

3.2. Sulfur poisoning

3.2.1. Morphology and crystal phase

Specific surface areas of the 1.0 wt% Pd/γ-Al_2O_3, 1.0 wt% Pd/10 wt% CeO_2/γ-Al_2O_3, and 1.0 wt% Pd/10 wt% $Ce_{0.6}Zr_{0.4}O_2/\gamma$-$Al_2O_3$ catalysts were 190, 181, and 180 $m^2\,g^{-1}$, respectively. After these catalysts were treated under a mixture of 5% SO_2–95% N_2 at 500 °C for 1.5 h, however, their corresponding specific surface areas decreased to 169, 175, and 163 $m^2\,g^{-1}$. The surface morphologies of the fresh and SO_2-poisoned catalysts were investigated by means of the TEM technique, and the results are presented in Fig. 4. The average particle sizes were 8–9 nm for the fresh three catalysts. The particle morphologies and sizes of the SO_2-poisoned catalysts remained almost unchanged as compared to those of the fresh counterparts, indicating that the treating of catalysts in a 5% SO_2–95% N_2 flow did not exert a significant effect on the surface morphology and particle size.

Fig. 5 shows the XRD patterns of the catalysts before and after methane combustion in the presence of 200 ppm SO_2 as well as of the catalyst after the SO_2-TPD experiment. In the fresh catalysts, there were no XRD peaks assignable to the PdO phase, which might be due to the low loading of Pd (1 wt%) and high dispersion of PdO on the surface of the catalyst. For the 1.0 wt% Pd/γ-Al_2O_3 catalyst after methane oxidation, XRD peaks at 2θ = 33, 45, 46, and 60° were observed, which could be ascribable to the $Al_2(SO_4)_3$ phase (JCPDS PDF# 81-1835). After loading 10 wt% CeO_2 or $Ce_{0.4}Zr_{0.6}O_2$ onto Pd/γ-Al_2O_3, however, the intensities of peaks attributed to the $Al_2(SO_4)_3$ phase were reduced for the $Pd/CeO_2/\gamma$-Al_2O_3 and $Pd/Ce_{0.6}Zr_{0.4}O_2/\gamma$-$Al_2O_3$ catalysts. One can see from Fig. 5 that the $Ce(SO_4)_2$ phase (JCPDS PDF# 22-0546) with the diffraction peaks at 2θ = 29, 33, 37, 40, 56, and 67° and the $Zr(SO_4)_2$ phase (JCPDS PDF# 72-2192) with the diffraction peaks at 2θ = 29, 36, 46, 56, and 60° could be found. Limousy et al. [24] showed that the adsorption of SO_2 on the Ce–Zr catalysts took place via the interaction with CeO_2 as described below:

$$6CeO_2 + 3SO_2 \rightarrow Ce_2(SO_4)_3 + 2Ce_2O_3$$

On the other hand, oxygen in the feed continuously reacted with Ce_2O_3 or $Ce_{0.6}Zr_{0.4}O_{2-x}$ to regenerate CeO_2 or $Ce_{0.6}Zr_{0.4}O_2$ that could release O atom to oxidize Pd^0 to form PdO active sites, companying by the $Ce^{4+} \leftrightarrow Ce^{3+}$ redox process. During the redox cycle of $CeO_2 \rightarrow Ce_2O_3 \rightarrow CeO_2$, the CeO_2 or $Ce_{0.6}Zr_{0.4}O_2$ particles would aggregate, causing a decrease in dispersion on the γ-Al_2O_3 support as a result. The poor dispersion of CeO_2 or $Ce_{0.6}Zr_{0.4}O_2$ after the above cycle could be proved by the rise in diffraction intensity of the CeO_2 or $Ce_{0.6}Zr_{0.4}O_2$ phase.

In the XRD profile (Fig. 5), the intensities of the peaks attributed to $Ce(SO_4)_2$ and $Zr(SO_4)_2$ phases were obviously stronger than that of the peaks due to the presence of $Al_2(SO_4)_3$. Because that the total conversion of $CeO_2 \rightarrow Ce(SO_4)_2$ and $ZrO_2 \rightarrow Zr(SO_4)_2$ only produced about 3.7 and 4.2 wt% weight increases for $Pd/CeO_2/\gamma$-Al_2O_3 and $Pd/Ce_{0.6}Zr_{0.4}O_2/\gamma$-$Al_2O_3$ catalysts, respectively, which were much lower than the saturation sulfur loading of 5–6 wt% for the two catalysts (see Section 3.3.1). We suspected that in the Ce-containing catalysts sulfur was absorbed mostly on the aluminum sites and formed aluminum sulfate that was highly dispersed on the surface of the catalysts and hardly detected by XRD technique. The presence of Ce promoted the removal of oxygen, which was a product of sulfate decomposition.

By comparing the XRD patterns of the SO_2-poisoned catalysts before and after the SO_2-TPD experiment, one can find that the XRD peaks of the sulfur-containing phases in the catalysts after SO_2-TPD experiment decreased in intensity, indicating that all of the sulfur-containing species could decompose at elevated temperature. In other words, the accumulation of sulfur in the catalysts could be suppressed as the reaction temperature increased.

3.2.2. Adsorption species and SO_2 desorption behavior

Fig. 6a shows the SO_2-TPD profiles of 1.0 wt% Pd/γ-Al_2O_3, 1.0 wt% Pd/10 wt% CeO_2/γ-Al_2O_3, and 1.0 wt% Pd/10 wt% $Ce_{0.6}Zr_{0.4}O_2/\gamma$-$Al_2O_3$ catalysts. All the catalysts gave two strong desorption peaks in the ranges of 130–200 °C and 600–950 °C. The peaks in the low-temperature range could be attributed to the desorption of weakly adsorbed SO_2, whereas those in the high-temperature region (above 600 °C) were due to the decomposition of sulfate species on the catalyst surfaces. For the 1.0 wt% Pd/γ-Al_2O_3 catalyst, the two SO_2 desorption peaks were at ca. 180 and 910 °C, respectively. When 10 wt% CeO_2 or 10 wt% $Ce_{0.6}Zr_{0.4}O_2$ was included in Pd/γ-Al_2O_3, the two SO_2 desorption peaks shifted to lower temperatures, suggesting that the decomposition of sulfate species on the surfaces of 1.0 wt% Pd/10 wt% CeO_2/γ-Al_2O_3 and 1.0 wt% Pd/10 wt% $Ce_{0.6}Zr_{0.4}O_2/\gamma$-$Al_2O_3$ was more facile than that on the surface of 1.0 wt% Pd/γ-Al_2O_3. In other words, the presence of Ce promoted the decomposition of the sulfate species. Waqif et al. [26] reported that the decomposition temperature of surface aluminum sulfate was 830 °C. Limousy et al. [24] observed that the bulk cerium sulfate and zirconium sulfate began to decompose at 600 and 670 °C, respectively. They also found that the presence of noble metals could decrease the decomposition temperature of zirconium sulfate to 630 °C. Similar phenomena were also observed in our present study. The desorption peak at ca. 910 °C over 1.0 wt% Pd/γ-Al_2O_3 could be attributed to the decomposition

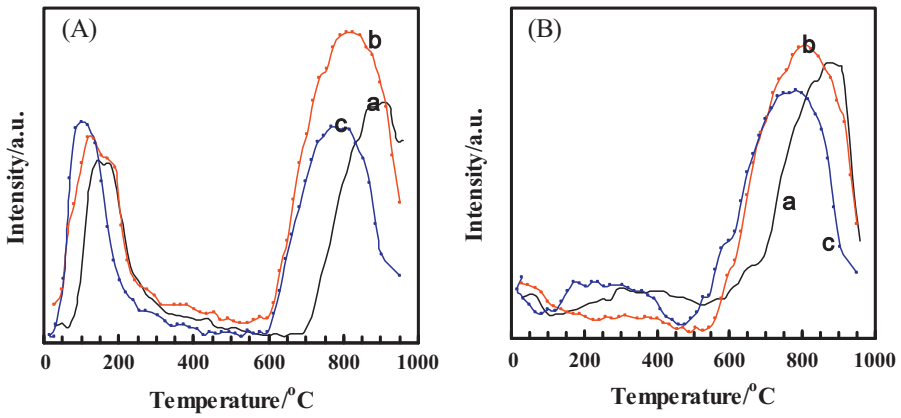

Fig. 6. (A) SO_2 and (B) O_2 signals the SO_2-TPD profiles of (a) Pd/γ-Al_2O_3, (b) Pd/CeO_2/γ-Al_2O_3, and (c) Pd/$Ce_{0.6}Zr_{0.4}O_2$/γ-Al_2O_3 catalysts.

of aluminum sulfate, whereas over the 1.0 wt% Pd/10 wt% CeO_2/γ-Al_2O_3 and 1.0 wt% Pd/10 wt% $Ce_{0.6}Zr_{0.4}O_2$/γ-Al_2O_3 catalysts, the SO_2 desorption peaks shifted to 820 and 766 °C, respectively, which was due to the decomposition of zirconium sulfate and/or cerium sulfate as well as the promotion of Ce for the aluminum sulfate decomposition either directly, or indirectly through its interaction with Pd. The onset decomposition temperature of sulfate species around 600 °C, coinciding with the temperature for the recovery of the catalytic activity (Figs. 2 and 3). The desorption peak area of the 1.0 wt% Pd/10 wt% CeO_2/γ-Al_2O_3 catalyst was obviously larger than those of the 1.0 wt% Pd/γ-Al_2O_3 and 1.0 wt% Pd/10 wt% $Ce_{0.6}Zr_{0.4}O_2$/γ-Al_2O_3 catalysts. This result suggests that more amount of sulfate species were formed on the 1.0 wt% Pd/10 wt% CeO_2/γ-Al_2O_3 catalyst. During the SO_2-TPD experiment, O_2 was also detected in the outlet gas at high temperature similar as that of SO_2 desorption at high temperature (Fig. 6b). It is not strange that no significant amount of O_2 was detected at low temperature since the desorption peaks of SO_2 at low temperature was due to the weakly adsorbed SO_2 on the catalyst surface. The desorption of SO_2 at high temperature occurred via the decomposition of surface sulfates according to the following reactions:

$$Al_2(SO_4)_3 \rightarrow Al_2O_3 + 3SO_2 + (3/2)O_2$$

$$Ce_2(SO_4)_3 \rightarrow Ce_2O_3 + 3SO_2 + (3/2)O_2$$

$$Ce(SO_4)_2 \rightarrow CeO_2 + 2SO_2 + O_2$$

$$Zr(SO_4)_2 \rightarrow ZrO_2 + 2SO_2 + O_2$$

Fig. 7 shows the SO_2-TPD profiles of the catalysts that were treated by a mixture of 5% H_2–95% N_2 at 500 °C for 2 h before the TPD test. A SO_2 desorption peak at low temperature (ca. 125 °C) could be observed over each of the three catalysts, and the peak intensity decreased in the order of the H_2-reduced 1.0 wt% Pd/10 wt% CeO_2/γ-Al_2O_3 > 1.0 wt% Pd/γ-Al_2O_3 > 1.0 wt% Pd/10 wt% $Ce_{0.6}Zr_{0.4}O_2$/γ-Al_2O_3 catalysts. At high temperature, however, no significant SO_2 desorption was observed over the 1.0 wt% Pd/γ-Al_2O_3 catalyst. Such phenomena could be explained as follows: PdO was active sites for the oxidation of SO_2 to give SO_3, and then to form surface sulfates; the reduction of PdO by H_2 was converted to Pd^0, the absence of active PdO species restrained the conversion of SO_2 to SO_3, and hence the surface sulfate species could not be generated, which resulted in the disappearance of SO_2 desorption peaks at high temperature. Interestingly, a weaker SO_2 desorption peak at ca. 715 °C appeared over the reduced Pd/CeO_2/γ-Al_2O_3 and Pd/$Ce_{0.6}Zr_{0.4}O_2$/γ-Al_2O_3 catalysts. Dai et al. [25] observed similar phenomena in both oxidizing and reducing circumstances. It can be explained that during the SO_2 adsorption process (in the flow of 5% SO_2–95% N_2 at 500 °C for 0.5 h), bulk oxygen in CeO_2 or $Ce_{0.6}Zr_{0.4}O_2$ diffused to the Pd active sites and then the Pd^0 was oxidized into PdO by converting Ce^{4+} to Ce^{3+}, which was in agreement with the results reported by other researchers [27,28]. Therefore, the SO_2 in the flow reacted with PdO to form sulfates, leading to a desorption signal at higher temperature in the SO_2-TPD profile. From Fig. 7, one can also see that the intensity of SO_2 desorption peak at high temperature over the reduced Pd/CeO_2/γ-Al_2O_3 catalyst was much higher than that over the reduced Pd/$Ce_{0.6}Zr_{0.4}O_2$/γ-Al_2O_3 catalyst. A similar trend is also observed in Fig. 6. It indicates that SO_2 is likely to react with CeO_2 to generate sulfates.

3.2.3. Surface chemical state

The XPS analyses of the used catalysts were carried out to investigate the relationship of surface species and valence state with the catalytic deactivation behavior. The Pd $3d_{5/2}$ XPS spectra of the catalysts after methane catalytic reaction in the presence of 200 ppm SO_2 and of the catalysts poisoned by SO_2 are illustrated in Fig. 8. It can be seen that the binding energy of Pd $3d_{5/2}$ of the catalysts pretreated in a mixture of 5% SO_2–95% N_2 (v/v, 50 ml min^{-1}) for 1.5 h was ca. 335.1 eV and that of Pd $3d_{5/2}$ of the catalysts after methane catalytic reaction in the presence of 200 ppm SO_2 was ca. 336.5 eV, which could be assigned to the surface Pd^0 and PdO species [24,29], respectively. As shown in Fig. 9, the binding energy of S 2p of the

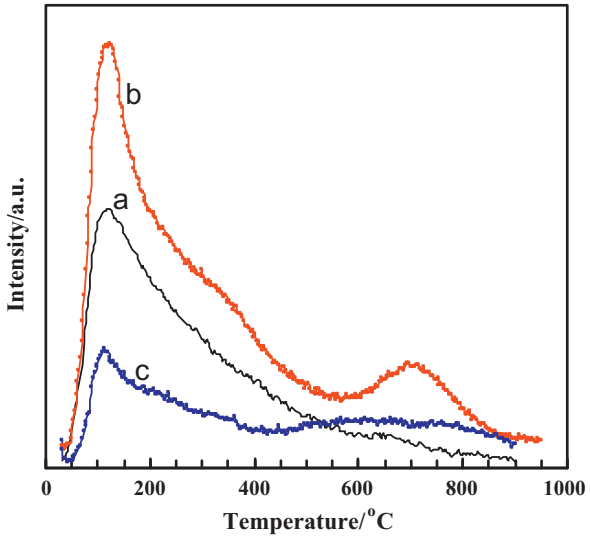

Fig. 7. SO_2-TPD profiles of the reduced Pd/γ-Al_2O_3 (a), Pd/CeO_2/γ-Al_2O_3 (b), and Pd/$Ce_{0.6}Zr_{0.4}O_2$/γ-Al_2O_3 (c) catalysts.

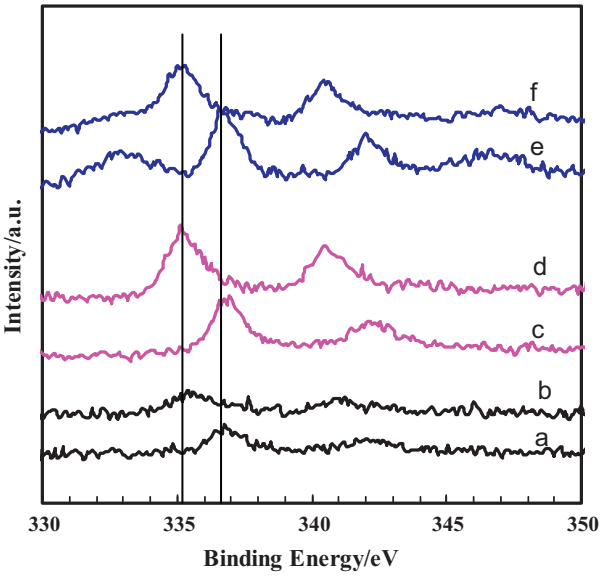

Fig. 8. Pd 3d XPS spectra of (a, b) Pd/Al_2O_3 (c, d) $Pd/CeO_2/Al_2O_3$, and (e, f) $Pd/Ce_{0.6}Zr_{0.4}O_2/Al_2O_3$ after (a, c, e) catalytic combustion of methane in the presence of 200 ppm SO_2 and (b, d, f) SO_2 pretreatments.

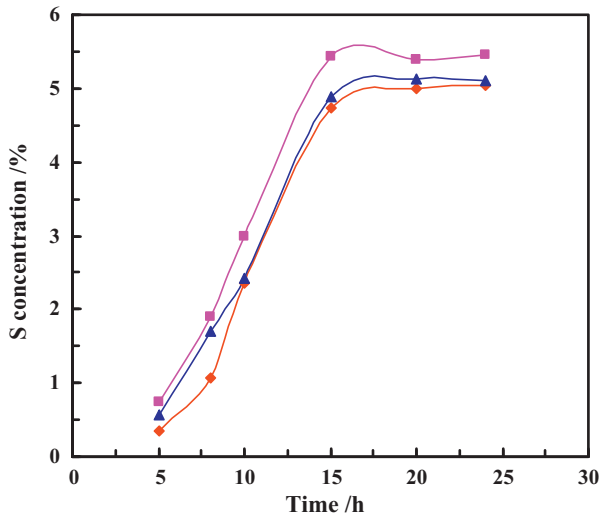

Fig. 10. S content in the (♦) $Pd/\gamma\text{-}Al_2O_3$, (■) $Pd/CeO_2/\gamma\text{-}Al_2O_3$, and (▲) $Pd/Ce_{0.6}Zr_{0.4}O_2/\gamma\text{-}Al_2O_3$ catalysts after SO_2 pretreatment for different time.

used catalysts was ca. 169 eV, indicating the presence of the sulfate species [24,30].

The presence of Pd^0 over the SO_2-poisoned catalysts was due to the fact that SO_2 was directly oxidized to SO_3 by PdO species, giving Pd^0 over the catalyst [24]. In the poisoning process, Pd^0 could not be oxidized to PdO because of the absence of oxygen in the gas flow, whereas in the catalytic combustion of methane, Pd^0 species were re-oxidized by the oxygen from gas-phase or from CeO_2 or $Ce_{0.6}Zr_{0.4}O_2$. The results of the catalytic activity and XPS investigations revealed that SO_2 might play an important role in the catalytic combustion of methane, and there were sulfur species formed on the catalyst surfaces when the reactant feed contained SO_2. The above discussion clearly explains the reasons for the sulfur poisoning and the decrease in methane catalytic combustion activity [13,23,31,32].

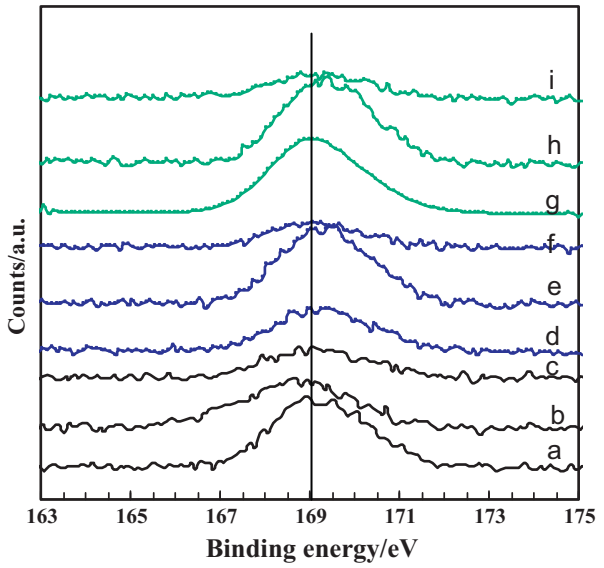

Fig. 9. S 2p XPS spectra of (a–c) Pd/Al_2O_3 (d–f) $Pd/CeO_2/Al_2O_3$, and (g–i) $Pd/Ce_{0.6}Zr_{0.4}O_2/Al_2O_3$ after (a, d, g) catalytic combustion of methane in the presence of 200 ppm SO_2, (b, e, h) SO_2 pretreatment, and (c, f, i) catalytic combustion of methane before which the catalysts were poisoned by SO_2.

3.3. Sulfur accumulation

The above results demonstrated that the formation of sulfate species from SO_2 resulted in the deactivation of the catalysts. The accumulation of sulfates during the reaction process is a key issue to affect the methane combustion activity of Pd-based catalyst. Therefore, we studied the accumulation of sulfates by treating the catalyst with a high concentration (5%) of SO_2 for different times, which was aimed to accelerate the sulfur poisoning process. For the SO_2-poisoned catalysts, we measured the sulfur concentration of the catalyst using a sulfur–carbon analyzer and investigated the decomposition of the surface sulfates by the DTA-TG apparatus.

3.3.1. Sulfur content analysis

Fig. 10 presents the sulfur contents of the catalysts as a function of treatment time in 5% SO_2 at 500 °C. With the increase in treatment time, the sulfur content in each of the three catalysts gradually increased to a constant level of ca.5–6 wt% after 18 h. Apparently, the sulfur saturation content of 1.0 wt% Pd/10 wt% $CeO_2/\gamma\text{-}Al_2O_3$ was higher than those of the other two catalysts. This result was in agreement with that of the SO_2-TPD studies (Fig. 6).

3.3.2. DTA-TG analysis

Fig. 11 shows the DTA-TG profiles of 1.0 wt% $Pd/\gamma\text{-}Al_2O_3$, 1.0 wt% Pd/10 wt% $CeO_2/\gamma\text{-}Al_2O_3$, and 1.0 wt% Pd/10 wt% $Ce_{0.6}Zr_{0.4}O_2/\gamma\text{-}Al_2O_3$ catalysts after 24 h treatment with 5% SO_2. All of the catalysts showed a weight loss at ca. 100 °C, which could be attributed to the desorption of SO_2 weakly adsorbed on the catalyst surfaces. The weight losses at 500 °C were due to the decomposition of surface sulfates [24]. Davis et al. [33] suggested that SO_3 was the primary decomposition product but it was not detected due to its rapid decomposition to SO_2 and O_2. The weight losses of the three catalysts tended to be flat after 1000 °C, implying that the sulfur species formed on the catalysts could be decomposed completely at high temperature (1000 °C). The weight losses due to the decomposition of sulfur species of the 1.0 wt% $Pd/\gamma\text{-}Al_2O_3$, 1.0 wt% Pd/10 wt% $CeO_2/\gamma\text{-}Al_2O_3$, and 1.0 wt% Pd/10 wt% $Ce_{0.6}Zr_{0.4}O_2/\gamma\text{-}Al_2O_3$ catalysts were 11.86, 14.53, and 11.95%, respectively. The weight losses were in good agreement with the sulfur contents determined by

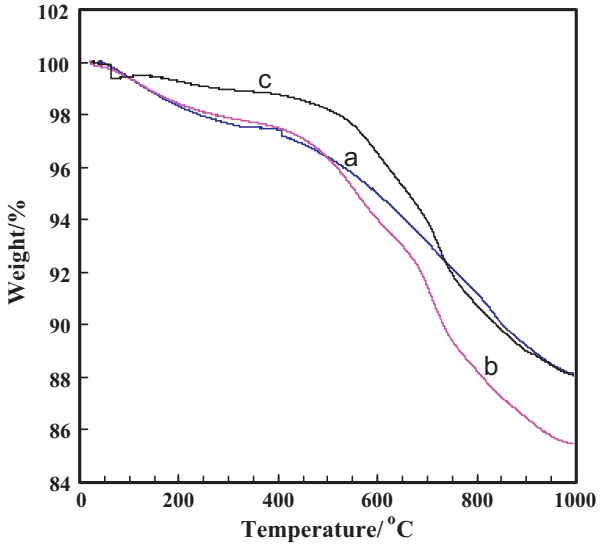

Fig. 11. TG curves of (a) $Pd/\gamma\text{-}Al_2O_3$, (b) $Pd/CeO_2/\gamma\text{-}Al_2O_3$, and (c) $Pd/Ce_{0.6}Zr_{0.4}O_2/\gamma\text{-}Al_2O_3$ after SO_2 pretreatment for 24 h.

the sulfur–carbon analyzer mentioned above, because the SO_2/SO_3 (M = 64/80) were the dominant desorption components and it was 2–2.5 times as much as the molecular weight of S element (M = 32).

4. Conclusions

The presence of SO_2 in the reaction gases had a negative effect on the activities of the Pd-based catalysts. Pretreatment of the catalysts with SO_2 also led to a decrease in catalytic activity to some extent. The sulfur poisoning and sulfate formation were mainly responsible for the catalyst deactivation. The PdO species contributed to the formation of sulfates by oxidizing SO_2 to SO_3 species. No obvious changes were found in the particle morphologies and sizes of the fresh and used catalysts. Sulfur accumulated to a constant concentration on the surfaces of each catalyst after treatment with 5% SO_2 after 18 h. The presence of CeO_2 or $Ce_{0.6}Zr_{0.4}O_2$ species in the catalysts lowered the decomposition temperature of sulfates to ca. 600 °C, indicating that the durability of the catalysts studied in this work could be satisfied for the catalytic combustion of methane that usually takes place above 800 °C.

Acknowledgements

This work was supported by the National Natural Science Foundation of China (Grant Nos. 20877006 and 20833011) and Natural Science Foundation of Beijing Municipality (Grant No. 2101002).

References

[1] R.A. Dalla Betta, T. Rostrup-Nielsen, Catal. Today 47 (1999) 369–375.
[2] R. Carroni, V. Schmidt, T. Griffin, Catal. Today 75 (2002) 287–295.
[3] P. Forzatti, Catal. Today 83 (2003) 3–18.
[4] D.D. Beck, J.W. Sommers, C.L. DiMaggio, Appl. Catal. B 11 (1997) 273–290.
[5] P. Gélin, M. Primet, Appl. Catal. B 39 (2002) 1–37.
[6] A. Trovarelli, C. de Leitenburg, M. Boaro, G. Dolcetti, Catal. Today 50 (1999) 353–367.
[7] S. Colussi, A. Trovarelli, G. Groppi, J. Llorca, Catal. Commun. 8 (2007) 1263–1266.
[8] M.L. Pisarello, V. Milt, M.A. Peralta, C.A. Querini, E.E. Mirò, Catal. Today 75 (2002) 465–470.
[9] M. Boaro, M. Vicario, C. de Leitenburg, G. Dolcetti, A. Trovarelli, Catal. Today 77 (2003) 407–417.
[10] L.S. Escandon, S. Ordóñez, A. Vega, F.V. Díez, Chemosphere 58 (2005) 9–17.
[11] S. Specchia, E. Finocchio, G. Busca, P. Palmisano, V. Specchia, J. Catal. 263 (2009) 134–145.
[12] S.W. Yang, A. Maroto-Valiente, M. Benito-Gonzalez, I. Rodríguez-Ramos, A. Guerrero-Ruiz, Appl. Catal. B 28 (2000) 223–233.
[13] S. Ordóñez, P. Hurtado, H. Sastre, F.V. Díez, Appl. Catal. A 259 (2004) 41–48.
[14] P. Hurtado, S. Ordóñez, H. Sastre, F.V. Díez, Appl. Catal. B 47 (2004) 85–93.
[15] N.S. Nasri, J.M. Jones, V.A. Dupont, A. Williams, Energy Fuels 12 (1998) 1130–1134.
[16] D.L. Mowery, M.S. Graboski, T.R. Ohno, R.L. McCormick, Appl. Catal. B 21 (1999) 157–169.
[17] L.J. Hoyos, H. Praliaud, M. Primet, Appl. Catal. A 98 (1993) 125–138.
[18] M. Waqif, J. Bachelier, O. Saur, J.C. Lavalley, J. Mol. Catal. 72 (1992) 127–138.
[19] J.K. Lampert, M.S. Kazi, R.J. Farrauto, Appl. Catal. B 14 (1997) 211–223.
[20] J. Mitome, G. Karakas, K.A. Bryan, U.S. Ozkan, Catal. Today 42 (1998) 3–11.
[21] D.L. Mowery, R.L. McCormick, Appl. Catal. B 34 (2001) 287–297.
[22] V. Meeyoo, D.L. Trimm, N.W. Cant, Appl. Catal. B 16 (1998) L101–L104.
[23] S. Ordóñez, P. Hurtado, F.V. Díez, Catal. Lett. 100 (2005) 27–34.
[24] L. Limousy, H. Mahzoul, J.F. Brilhac, P. Gilot, F. Garin, G. Maire, Appl. Catal. B 42 (2003) 237–249.
[25] Z.Y. Dai, Y. Li, Z.F. He, Z.G. Wang, Z.J. Da, Acta Petrol. Sin. 22 (2006) 1–5 (in Chinese).
[26] M. Waqif, O. Saur, J.C. Lavalley, Y. Wang, B.A. Morrow, Appl. Catal. 71 (1991) 319–331.
[27] C.A. Müller, M. Maciejewski, R.A. Koeppel, A. Baiker, Catal. Today 47 (1999) 245–252.
[28] R. Burch, P.K. Loader, Appl. Catal. B 5 (1994) 149–164.
[29] O. Demoulin, B.L. Clef, M. Navez, P. Ruiz, Appl. Catal. A 344 (2008) 1–9.
[30] E.J. Romano, K.H. Schulz, Appl. Surf. Sci. 246 (2005) 262–270.
[31] J.M. Jones, V.A. Dupont, R. Brydson, D.J. Fullerton, N.S. Nasri, A.B. Ross, A.V.K. Westwood, Catal. Today 81 (2003) 589–601.
[32] P. Gélin, L. Urfels, M. Primet, E. Tena, Catal. Today 83 (2003) 45–57.
[33] B.H. Davis, R.A. Keogh, R. Srinivasan, Catal. Today 20 (1994) 219–256.